

Shallow geophysical imaging of the Olympia anomaly: An enigmatic structure in the southern Puget Lowland, Washington State

Jack K. Odum¹, William J. Stephenson¹, Thomas L. Pratt², and Richard J. Blakely³

¹Geologic Hazards Science Center, U.S. Geological Survey, PO Box 25046, MS 966, Denver, Colorado 80225, USA

²U.S. Geological Survey, 12201 Sunrise Valley Drive, MS 905, Reston, Virginia 20192, USA

³U.S. Geological Survey, 345 Middlefield Road, MS 989, Menlo Park, California 94025, USA

ABSTRACT

Gravity and magnetic anomalies suggest that the Olympia structure beneath the southern Puget Lowland (western Washington State, U.S.) vertically displaces Eocene Crescent Formation strata. Northeast of the Olympia structure, middle Eocene Crescent Formation is beneath 4–6 km of Paleogene–Neogene and Quaternary strata of the Tacoma basin, whereas the Crescent Formation is exposed at the surface immediately to the south. Although numerous marine seismic reflection profiles have been acquired near the surface location of the Olympia structure as defined by potential field anomalies, its tectonic character remains enigmatic, in part because inlets of southern Puget Sound are too shallow for the collection of deep-penetration marine seismic profiles across the geophysical anomalies. To supplement existing shallow-marine data near the structure, we acquired 14.6 km of land-based seismic reflection data along a profile that extends from Crescent Formation exposed in the Black Hills northward across the projected surface location of the Olympia structure. The reflection seismic data image the Crescent bedrock surface to ~1 km depth beneath the southern Tacoma basin and reveal the dip on this surface to be no greater than ~10°. Although regional potential field data show a strong linear trend for the Olympia structure that implies folding over a blind thrust and/or bedrock juxtaposed against a weakly to nonmagnetic sediment section, high-resolution magnetic anomaly analysis along the land-based profile suggests that the structure is more complex. Overall, seismic and potential-field profiles presented in this study identify only minor shallow faulting within the projected surface location of the Olympia structure. We suggest that the mapped trace of the Olympia structure along the northern flank of the Black Hills, at least within the study area, is constrained by juxtaposed normal and reversely magnetized Crescent Formation units and minor tectonic deformation of Crescent Formation bedrock.

INTRODUCTION

The Puget Lowland of western Washington State is home to more than three million people in major urban centers such as Seattle, Tacoma, and Olympia, and has some of the nation's largest ports, air facilities, military

bases, and high-tech industries. The complex tectonic structure in the region results from the oblique northeast-directed subduction of the Juan de Fuca oceanic plate beneath western North America (Fig. 1A), northwest motion of the Pacific plate along the San Andreas fault system, and clockwise rotation and northward motion of the Coast Range block (Wells et al., 1998; Wells and Simpson, 2001; Blakely et al., 2002; Van Wagoner et al., 2002; Johnson et al., 2004; McCaffrey et al., 2007, 2013). The convergence of the Juan de Fuca plate, at a rate of ~50 mm/yr (Atwater, 1970; DeMets et al., 1994), has historically produced great (magnitude, M8–9) earthquakes on the Cascadia subduction zone (e.g., Nelson et al., 2006) that pose a primary seismic hazard for the region (Petersen et al., 2002). In the Puget Lowland, north-south compression causes 4.4 ± 0.3 mm/yr of permanent shortening (Mazzotti et al., 2002; McCaffrey et al., 2007) that is accommodated in part by a series of east- and southeast-striking folds and faults that cross the lowland. These crustal faults within the North American plate also pose a substantial seismic hazard and, because of their proximity to large cities, may pose more of a risk than large subduction-zone events (Petersen et al., 2002). Paleoseismic studies in the Puget Lowland document uplifted shorelines, Holocene fault scarps, abrupt subsidence of tidal marshes, and tsunami deposits, all indicating that M7 or greater earthquakes have occurred on shallow faults within the Seattle and Tacoma fault zones (Figs. 1B, 1C) (e.g., Atwater and Moore, 1992; Bucknam et al., 1992; Sherrod, 2001; Nelson et al., 2003, 2014; Booth et al., 2004; Kelsey et al., 2004, 2008; Blakely et al., 2009, 2011; Mace and Keranen, 2012; Barnett et al., 2015). These crustal faults remain the subject of debate because their location, geometry, and slip rates have not been well constrained, resulting in contrasting kinematic models (e.g., Pratt et al., 1997, 2015; Johnson et al., 1999; ten Brink et al., 2002; Brocher et al., 2001, 2004; Kelsey et al., 2008; Liberty and Pratt, 2008).

Black Hills Uplift and the Olympia Structure

The Black Hills are one of the largest uplifted exposures of basement rocks in the area surrounding the Puget Lowland. Uplift began in the early or middle Eocene, based on the stratigraphic relationship between onlapping latest Eocene to Oligocene sediments on the west and south sides of the Black Hills and evidence for the influence of an uplifted Black Hills on basin sedimentation

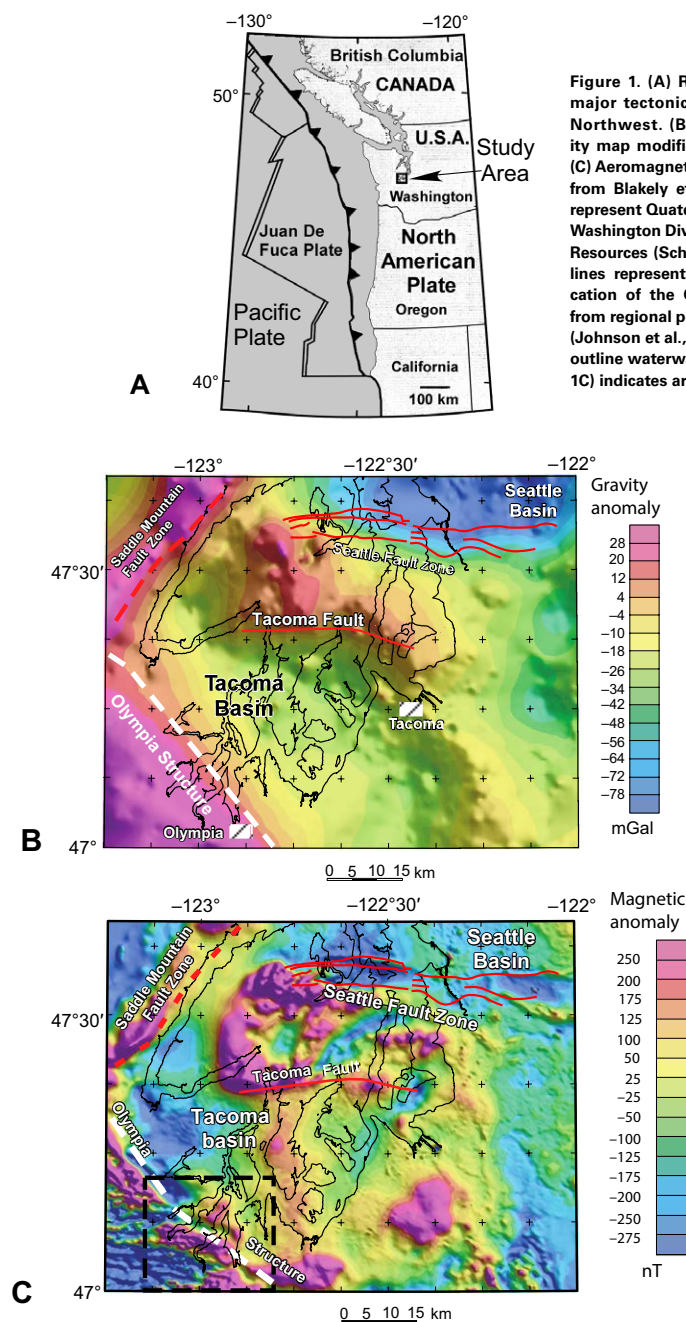


Figure 1. (A) Regional setting showing major tectonic structures in the Pacific Northwest. (B) Isostatic residual gravity map modified from Finn et al. (1991). (C) Aeromagnetic anomaly map (modified from Blakely et al., 1999). Thin red lines represent Quaternary faults modified from Washington Division of Geology and Earth Resources (Schuster, 2005). Dashed white lines represent the surface projected location of the Olympia structure defined from regional potential field interpretation (Johnson et al., 2004). Black lines on maps outline waterways. Black dashed box (Fig. 1C) indicates area of study.

to the west (Walsh et al., 1987, 2003; Logan and Walsh, 2004). Eocene uplift of the Black Hills is consistent with documented uplift and northwest-trending anticlinal folding of thrust fault- and reverse fault-bound crustal blocks to the south and southeast of the Black Hills beginning in the middle Eocene (Globerman et al., 1982; Wells and Coe, 1985; Stanley et al., 1994, 1996). Also beginning in the middle Eocene, the development of dextral strike-slip displacement along and across discrete crustal blocks played a significant role in the accommodation of transpression associated with oblique plate subduction (Wells and Coe, 1985; Stanley et al., 1996).

The least studied of the known major structures beneath the Puget Lowland is the Olympia structure, the surface projection of which along the northeast flank of the Black Hills is located solely on the basis of potential field interpretations (Figs. 1B, 1C, and 2A). The Olympia structure is defined on the basis of pronounced northwest-southeast-trending geophysical anomalies that coincide with the southern margin of the Tacoma basin and northeast edge of the Black Hills uplift. Evidence for subsidence, presumably caused by a large earthquake ~1100 yr ago, is found near the anomaly traces, but a specific causative fault has not been identified (Sherrod, 2001; Nelson et al., 2014). In this paper we present a shallow integrated geophysical study that crosses the trace of the Olympia structure near Olympia, Washington. Our study utilizes a newly acquired 14.6-km-long land-based high-resolution seismic reflection profile, newly developed regional and site-specific magnetic and gravity analyses, and reexamination of earlier marine seismic profiles. We use these data to examine the character of shallow (≤ 1 km depth) deformation associated with the sharp and well-defined Olympia structure lineament.

GEOLOGICAL AND GEOPHYSICAL BACKGROUND

The Puget Lowland is a broad forearc valley that overlies a major north-trending crustal boundary between Paleocene–Eocene basement rocks of the Coast Range province to the west and pre-Tertiary (i.e., Paleogene–Neogene) rocks of the Cascade province to the east. The Coast Range basement rocks beneath the southern Puget Lowland consist of Paleocene to early Eocene Crescent Formation basaltic rocks and sedimentary strata believed to be similar to rocks exposed in adjacent uplifts of the western Olympic Mountains and Black Hills (Wells et al., 2014). The Crescent Formation is composed of a thick sequence of basalt flows and breccia, with minor interbeds of sedimentary rocks, formed in a continental-margin rift or island-arc setting (Globerman et al., 1982; Wells and Coe, 1985; Babcock et al., 1992; Wells et al., 2014). The Crescent Formation and its southern equivalent, the Siletz River volcanic rocks, are anomalously thick volcanic units. Modeling of magnetotelluric profiles in southwest Washington State indicates a thickness of 20 km or more (Stanley et al., 1996); gravity models suggest thicknesses of as much as 30 km (Finn, 1990); seismic reflection data indicate as much as 33 km in Oregon thinning to 20 km in Washington (Tréhu et al., 1994); tomographic imaging using earthquake data suggests 25 km of Coast Range rocks beneath the Puget Lowland

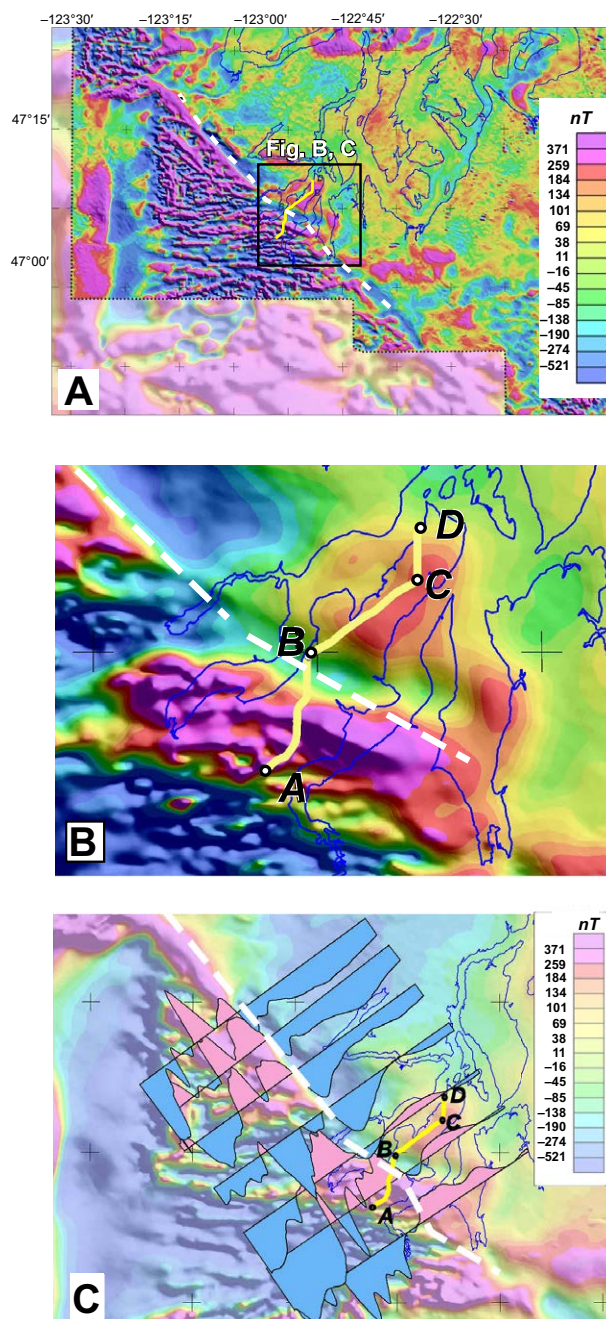


Figure 2. (A) Regional aeromagnetic anomalies map, filtered to emphasize shallow sources. Lower resolution data shown as dimmed image. Yellow line is the Steamboat Island Road (SI) land-based seismic reflection profile (Figs. 4 and 6). (B) Close-up view of study area indicated by black box in A. Letters A–D represent reference points along aeromagnetic value graph (Fig. 7B) and SI seismic profile (Fig. 7C) that are discussed in text. White dashed line represents the surface projected location of the Olympia structure based on regional potential field interpretation (Fig. 1C). (C) Blue and pink profiles digitized from the original aeromagnetic data. Profiles show the variation in magnetic value of basement rock (Crescent Formation) related to depth of burial beneath non-magnetic sediments and changing physical properties, including reversed magnetization, of the volcanic basement rock.

(Lees and Crosson, 1990); and Babcock et al. (1992) described a 16.2 km thickness of Crescent Formation rocks on the eastern flank of the Olympic Peninsula.

Large areas of the Puget Lowland are covered by waterways, urban development, dense forests, and thick sequences of glacial and postglacial deposits that conceal or subdue the surface expression of active faults and folds. Most of what is known about the subsurface structure beneath the Puget Lowland comes from potential field surveys and seismic studies (Figs. 1B, 1C; e.g., Daneš et al., 1965; Gower et al., 1985; Finn, 1990; Finn et al., 1991; Johnson et al., 1994, 1999; Snively and Wells, 1996; Pratt et al., 1997; Brocher et al., 2001, 2004; Blakely et al., 2011; Lamb et al., 2012; Mace and Keranen, 2012). In the Puget Lowland region, these geophysical data indicate that north-south compression has deformed the forearc basement and overlying Quaternary and older rocks into a series of fault- or fold-bounded basins and uplifts (e.g., Gower et al., 1985; Pratt et al., 1997; Brocher et al., 2001; Van Wagoner et al., 2002; Kelsey et al., 2008; Liberty and Pratt, 2008; Blakely et al., 2009; Mace and Keranen, 2012).

Originally defined by linear gravity and magnetic anomalies, the Olympia structure is ~80 km long with a trend of ~315° (Finn, 1990; Finn et al., 1991; Blakely et al., 1999). The linearity of the potential field gradients and results from tomographic analyses suggest that the Olympia structure is a fold or fault that separates uplifted Crescent Formation basement rock exposed in the Black Hills south of the structure from basement rock buried 3.5–6.0 km beneath sedimentary strata of the Tacoma basin to the north (Figs. 1B, 1C; Pratt et al., 1997; Brocher et al., 2001). Unfortunately, existing two- and three-dimensional tomographic models do not properly image the Olympia structure because they rely heavily on seismic sources from marine reflection profiling in waterways north of the structure, and on earthquake sources that are sparse south of the structure (Brocher et al., 2001; Van Wagoner et al., 2002).

The tectonic character of the Olympia structure has remained enigmatic because the shallow and constricted waterways of southern Puget Sound have prevented the collection of deep-penetration marine seismic reflection profiles across the projected trace of the geophysical anomalies (Pratt et al., 1997). Only higher resolution shallow-marine seismic profiles collected with small sources (sparkers and airguns) and limited receiver aperture (sometimes only single channel) have been collected in the southern inlets near Olympia, and these have not imaged the Olympia structure (Johnson et al., 2004; Clement et al., 2010). The marine seismic reflection profiles were summarized in Pratt et al. (1997) and Clement et al. (2010). Our study uses the industry profile Western 36 interpretation (of Pratt et al., 1997) of a gently north-dipping Crescent Formation basement surface north of the Olympia structure; however, this deep seismic profile did not extend far enough south to cross the surface projection

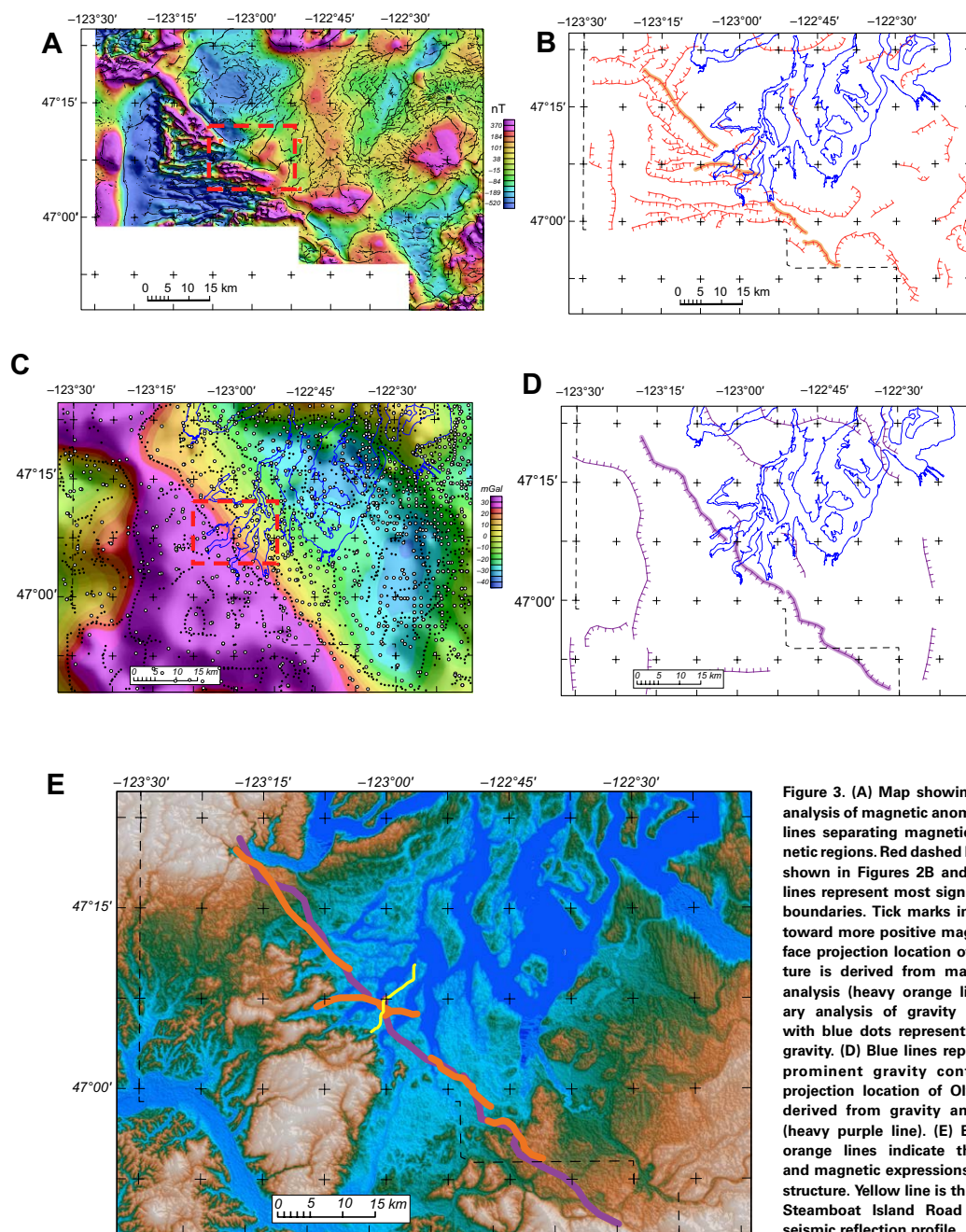


Figure 3. (A) Map showing the boundary analysis of magnetic anomalies with black lines separating magnetic and less magnetic regions. Red dashed box is study area shown in Figures 2B and 4. (B) Thin red lines represent most significant magnetic boundaries. Tick marks indicate direction toward more positive magnetization. Surface projection location of Olympia structure is derived from magnetic anomaly analysis (heavy orange line). (C) Boundary analysis of gravity anomalies map with blue dots representing contrasts in gravity. (D) Blue lines represent the most prominent gravity contrasts. Surface projection location of Olympia structure derived from gravity anomaly analysis (heavy purple line). (E) Bold purple and orange lines indicate the gravitational and magnetic expressions of the Olympia structure. Yellow line is the location of the Steamboat Island Road high-resolution seismic reflection profile.

of the Olympia structure as defined by potential-field anomaly gradients. The high-resolution marine seismic profiles show a disrupted zone of faulted and folded strata possibly related to the Olympia structure, but the profiles do not penetrate deeply enough, ≤ 1.5 km, to image any broader underlying fault system. Magsino et al. (2003) collected high-resolution gravity and ground magnetic data along 3 traverses, 35 km apart and orthogonal to the strike of the Olympia structure. Preliminary analyses of these traverses showed a relatively consistent ≥ 90 mGal gravity anomaly between the Black Hills and Tacoma basin. However, detailed modeling was unable to determine whether the gravity and magnetic anomalies reflect faults or folds (Magsino et al., 2003). Paleoseismic evidence of Holocene land-level changes along the trends of the Tacoma fault zone and Olympia structure suggests that a large earthquake (source fault unknown) caused land-level changes ~ 1100 yr ago in the southern Puget Lowland (Bucknam et al., 1992; Sherrod, 2001; Sherrod et al., 2000, 2004; Nelson et al., 2014; Barnett et al., 2015).

AEROMAGNETIC AND GRAVITY ANALYSIS

Figure 1C shows high-resolution aeromagnetic anomalies of the Puget Lowland acquired by fixed-wing aircraft in 1997 (Blakely et al., 1999). The airborne survey was flown as close to the ground as safely possible, nominally at 300 m above terrain, along north-south flight lines spaced 400 m apart, and along east-west tie lines spaced 4 km apart. A stationary magnetometer was operated during the survey to measure and subsequently correct for time varying magnetic fields. Total-field measurements were converted to total-field anomalies by subtraction of the International Geomagnetic Reference Field. Figure 2A shows the southern portion of these aeromagnetic data filtered to emphasize shallow magnetic sources. This was accomplished by analytically continuing the original data to a slightly higher (50 m) observation surface, then subtracting that result from the original data, effectively simulating a discrete vertical derivative (Blakely, 1995).

The northwest-striking Olympia structure marks a stark change in the pattern of magnetic anomalies (Fig. 2A). Southwest of the Olympia structure, anomalies display high amplitudes and short wavelengths, indicative of shallow magnetic sources, whereas anomalies northeast of the structure are broad and lower in amplitude, suggesting deeper magnetic sources. The change in wavenumber content is particularly evident in magnetic anomalies filtered to emphasize shallow magnetic sources (Fig. 2A). The mapped location of the Olympia structure is often shown in the literature (e.g., Johnson et al., 2004) as a continuous line. It is evident from Figures 2B and 2C, however, that the structure has significant complexity.

Figure 3A shows contacts between magnetic and less magnetic regions, determined with a three-step procedure. First the magnetic anomalies were converted to pseudogravity anomalies, an operation that includes reduction to the pole (Blakely, 1995). The maximum horizontal gradient of the pseudogravity field was then calculated, and mathematical curvature analysis was

used to locate gradient maxima (Blakely and Simpson, 1986; Phillips et al., 2007). This three-step methodology provides the location of abrupt lateral variations in crustal magnetization, shown as sinuous alignments of black dots in Figure 3A. This method assumes that contacts are vertical; dipping contacts will displace the boundaries slightly. Our interpretation of the location of the surface projection of the Olympia structure on the basis of the magnetic boundary analysis is shown by the orange lines in Figure 3B.

Figure 1B shows regional isostatic residual gravity anomalies modified from Simpson et al. (1986). A boundary analysis of the gravity anomalies is shown in Figure 3C; blue dots mark contacts between areas of more dense and less dense rocks. Density contacts are calculated using the same methodology described for the magnetic boundary analysis, but without the conversion to pseudogravity (Blakely and Simpson, 1986). The bold purple line in Figure 3D represents our objective interpretation of the location of the surface projection of the Olympia structure based on gravity anomalies.

In our view, the mapped location of the Olympia structure as independently determined from gravity and magnetic anomalies is remarkably consistent (Fig. 3E), although the gravitational expression of the Olympia structure is somewhat simpler than the magnetic expression for various reasons. First, gravity anomalies are by nature smoother than magnetic anomalies (Blakely, 1995). Second, magnetic anomalies emphasize shallower parts of the crust as compared to gravity anomalies. Third, gravity data in this location are more sparsely distributed than the detailed aeromagnetic flight-line data. Fourth, rock density varies by 25% at most, whereas rock magnetization varies by orders of magnitude and often switches polarity. While the gravity and magnetic interpretations are consistent, it is also clear that the Olympia structure is not a simple straight-line feature.

SEISMIC REFLECTION IMAGING OF THE OLYMPIA STRUCTURE

High-Resolution Marine Seismic Profiles

Several high-resolution marine seismic reflection profiles have been collected in Budd and Eld Inlets within the vicinity of the inferred surface location of the Olympia structure (Fig. 4). Two marine profiles imaging to ~1 km depth (P292-294 and P300-301) were acquired as part of the cruise described by Johnson et al. (2004). The data were presented in Clement et al. (2010). In addition to these previously published data, another small airgun profile was collected in Budd Inlet (P289-291; location shown in Fig. 4) as part of the Johnson et al. (2004) cruise, and is presented for the first time here. These profiles used a short recording streamer, so they do not provide effective velocity control and are therefore similar to single-channel data. All of these marine profiles are available on a U.S. Geological Survey website (<http://walrus.wr.usgs.gov/infobank/g/g297ps/html/g-2-97-ps.meta.html>). In the absence of reliable velocity control, we migrated the profiles using a velocity function suitable for sedimentary strata and broadly consistent with tomography models (Brocher

et al., 2001; Van Wagoner et al., 2002) in the Puget Lowland region. All three of the Budd and Eld Inlet marine profiles show gently north-dipping reflectors to ~1 km depth without prominent unconformities (Fig. 5). Clement et al. (2010) used high-resolution data collected with a small sparker source to describe an ~2-km-wide zone of shallow strata that are disrupted and gently folded near the mouths of Budd and Eld Inlets (profiles P292-294 and P300-30), and a similar zone is observed on the previously unpublished Budd Inlet profile P289-291. These deformed zones are represented with a hachured bar pattern on the Figure 4 seismic profile location map and the seismic profiles (Fig. 5). Near the southern end of these zones of deformation Clement et al. (2010) used sag features, transparent zones, and minor reflector offset to interpret apparent nearly vertical faults (black dashed lines in Fig. 5) that appear to disrupt the shallowest resolved reflectors; we also interpret these features on all three seismic profiles.

Steamboat Island Road Profile

To characterize the Olympia structure south of where marine profiles have been collected, we acquired a 14.6-km-long high-resolution P-wave seismic reflection profile along Steamboat Island Road, on a northeast-trending peninsula between Totten and Eld Inlets northwest of Olympia (Fig. 4). This profile extends from outcrops of Crescent Formation rocks south of U.S. Highway 101, northward onto Tacoma basin strata. The Steamboat Island Road (SI) seismic reflection profile was acquired using a minivibe seismic source and a 192 channel geophone array with 5 m source and receiver intervals (typically 960 m maximum aperture). The minivibe source swept linearly from 15 to 160 Hz over a 12 s interval, and we recorded data on 8 Hz P-wave vertical sensors. The seismic processing was mostly conventional, including amplitude corrections, bandpass filtering, and multiple passes of both residual statics corrections and stacking velocity analysis. However, we also applied less conventional processing steps, including precorrelation automatic gain correction and prestack dip filtering, to further mitigate noise caused by vehicle traffic along the roadway. The seismic section was post-stack migrated with an explicit finite-difference scheme, then converted to depth using a smoothed final stacking velocity function. The nominal vertical resolution throughout the upper 600 m is between 4 and 9 m.

Western 36 is an industry marine profile acquired northeast of Budd Inlet that ended ~2 km northeast of the land-based SI profile. The Western 36 profile was collected using a single-channel streamer because of the shallow, restricted waterways, but nonetheless imaged to a depth of ~2 km, although without constraint from velocity analysis (Pratt et al., 1997). The combined Western 36 marine and SI land profiles form an ~26-km-long image of bedrock (Crescent Formation surface) and overlying strata across the southern Tacoma basin and the trace of the Olympia structure, with a 2 km gap between them when projected onto a northeast-trending profile (Figs. 4 and 6). Figures 6A (uninterpreted) and 6B (interpreted) present the migrated and depth converted SI and Western 36 profiles at a vertical exaggeration of 4:1.

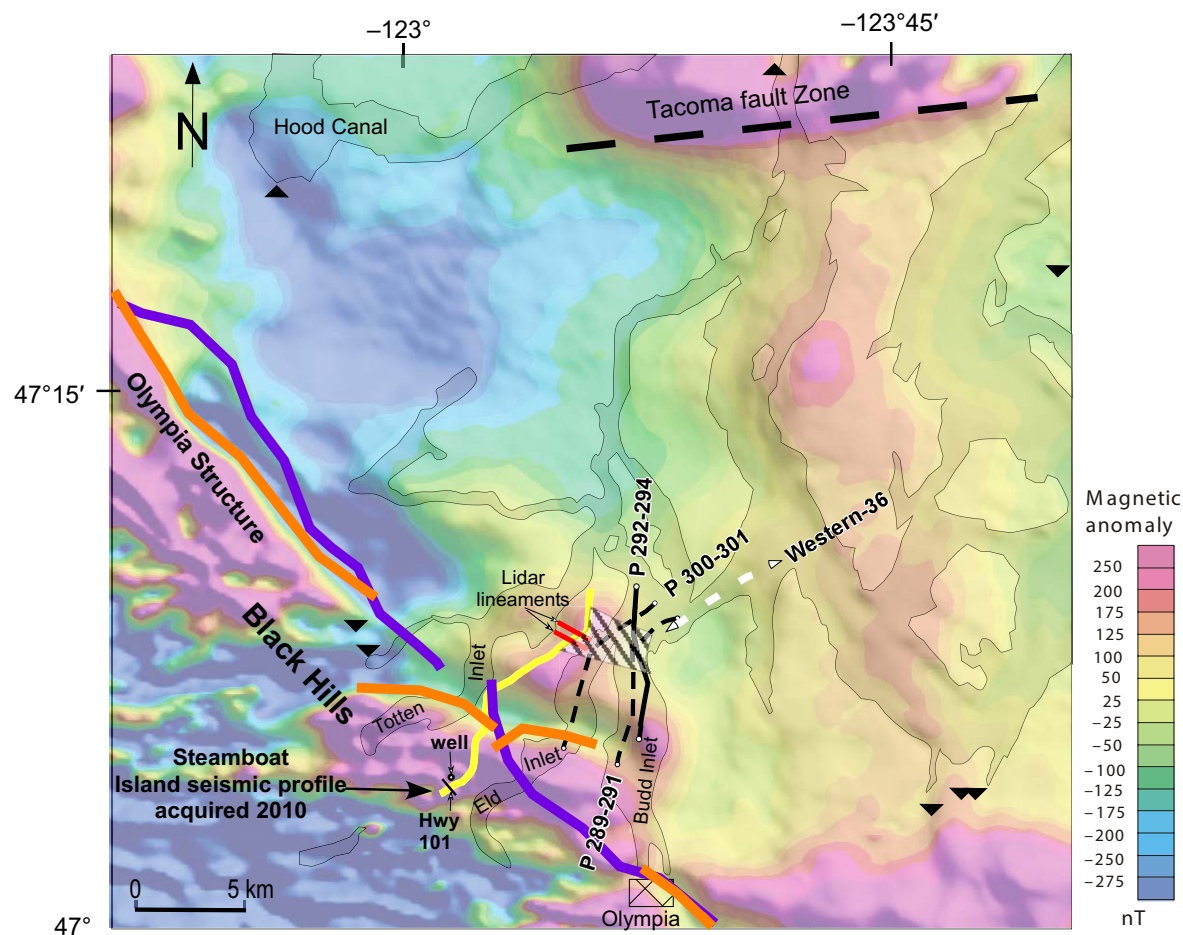





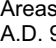
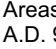


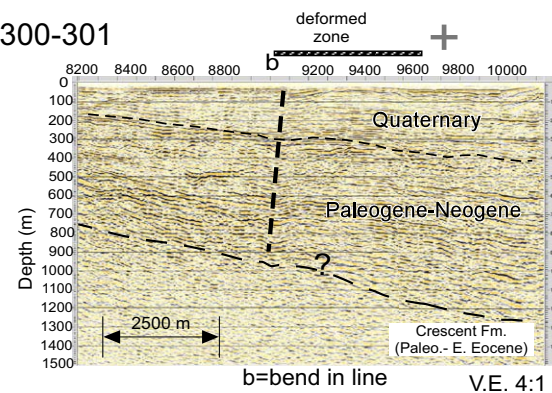


Figure 4. Projected on a section of the magnetic anomaly map shown in Figure 1C are the spatial locations of marine (black dashed and solid lines) and land-based Steamboat Island Road seismic reflection profiles (yellow line) that cross, or are in the vicinity, of the Olympia structure location derived from gravity (thick purple line) and aeromagnetic (thick orange line) boundary analysis (Figs. 3A–3E). Lidar—light detection and ranging.

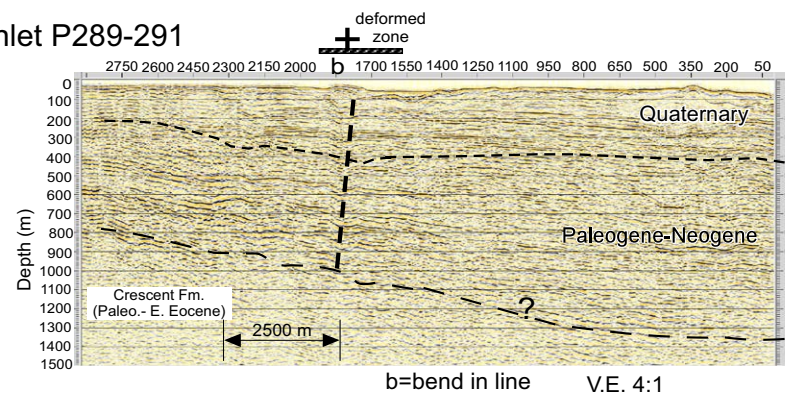
-  Steamboat Island Road seismic reflection profile, minivibe source, 5 m geophone spacing (this paper)
-  Single-fold marine seismic reflection profile (Pratt et al., 1997)
-  Migrated, multichannel marine seismic reflection profile (unpublished)
-  Surface location of the Olympia structure as defined by new magnetic (orange) and gravity (purple) anomaly models (this paper)
-  Migrated, multichannel marine seismic reflection profile (Clement et al., 2010).
-  Areas of earthquake-induced subsidence about A.D. 900. (Sherrod, 2001).
-  Areas of earthquake-induced uplift about A.D. 900 (Sherrod et al., 2004).
-  Zone of shallow reflector disruption interpreted from high-resolution seismic reflection profiles
-  Lidar lineaments (Clement et al., 2010)

Eld Inlet P300-301

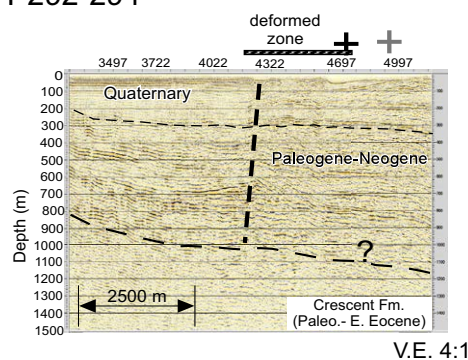


A

Budd Inlet P289-291



Budd Inlet P292-294



B= bend in profile

✚ Profile P 292-294 crosses profile P 289-291

✚ Profile P292-294 crosses P300-301 at gray cross.

✚ See Figure 4.

▨ Zone of wavy and disrupted reflectors.

Figure 5 (on this and following page). (A) Single channel Eld and Budd Inlet marine seismic reflection marine profiles modified from Clement et al. (2010). Profile P289-291 is a previously unpublished survey segment located west of Budd Inlet profile P292-294 acquired by Johnson et al. (2004); see Figure 4 for location. Crosses indicate points where profile P292-294 intersects the other Budd and Eld Inlet profiles (Fig. 4). Hachured bands represent areas of reflector deformation and suspected faulting from Clement et al. (2010) and this study. V.E.—vertical exaggeration; Fm—formation.

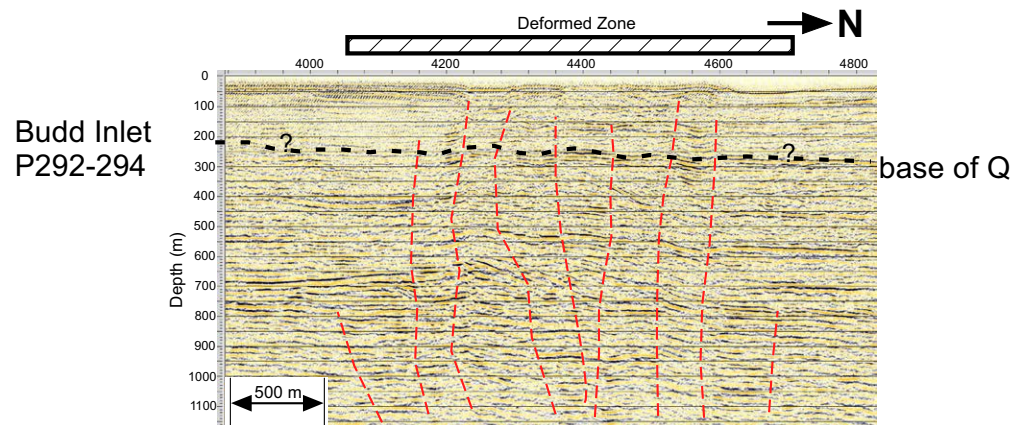
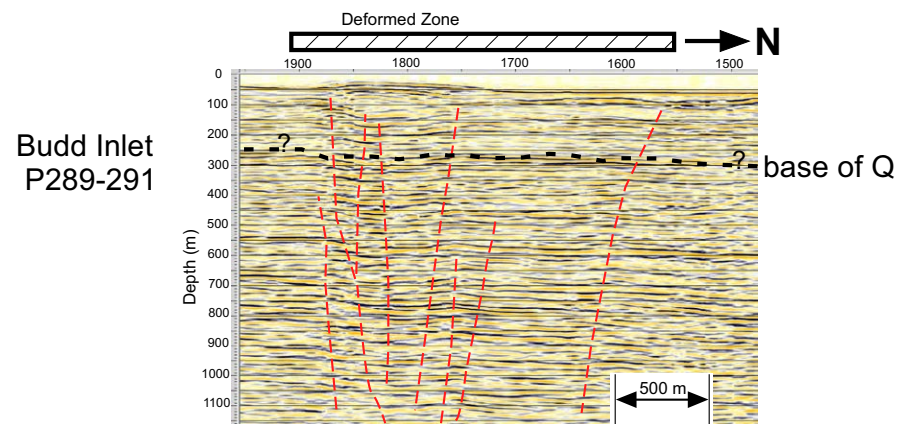
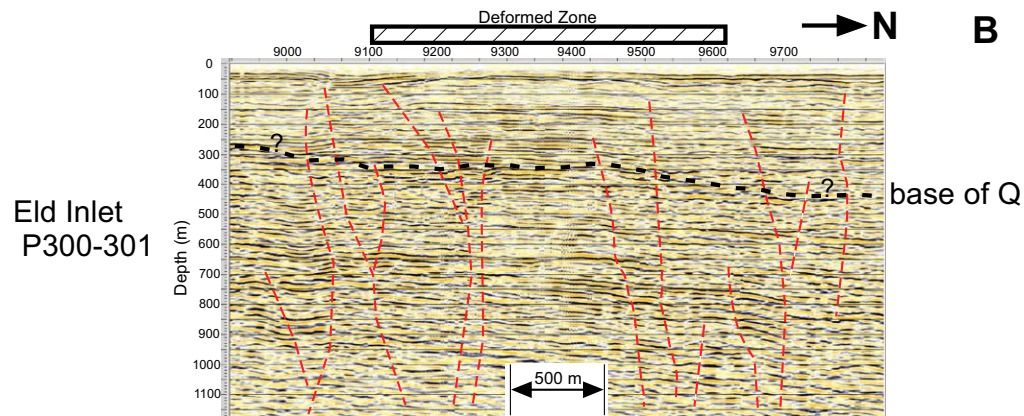


Figure 5 (*continued*). (B) Close-up view of deformed zones identified on the marine seismic profiles (Fig. 5A) showing minor faulting and reflector disruption. Q—Quaternary.

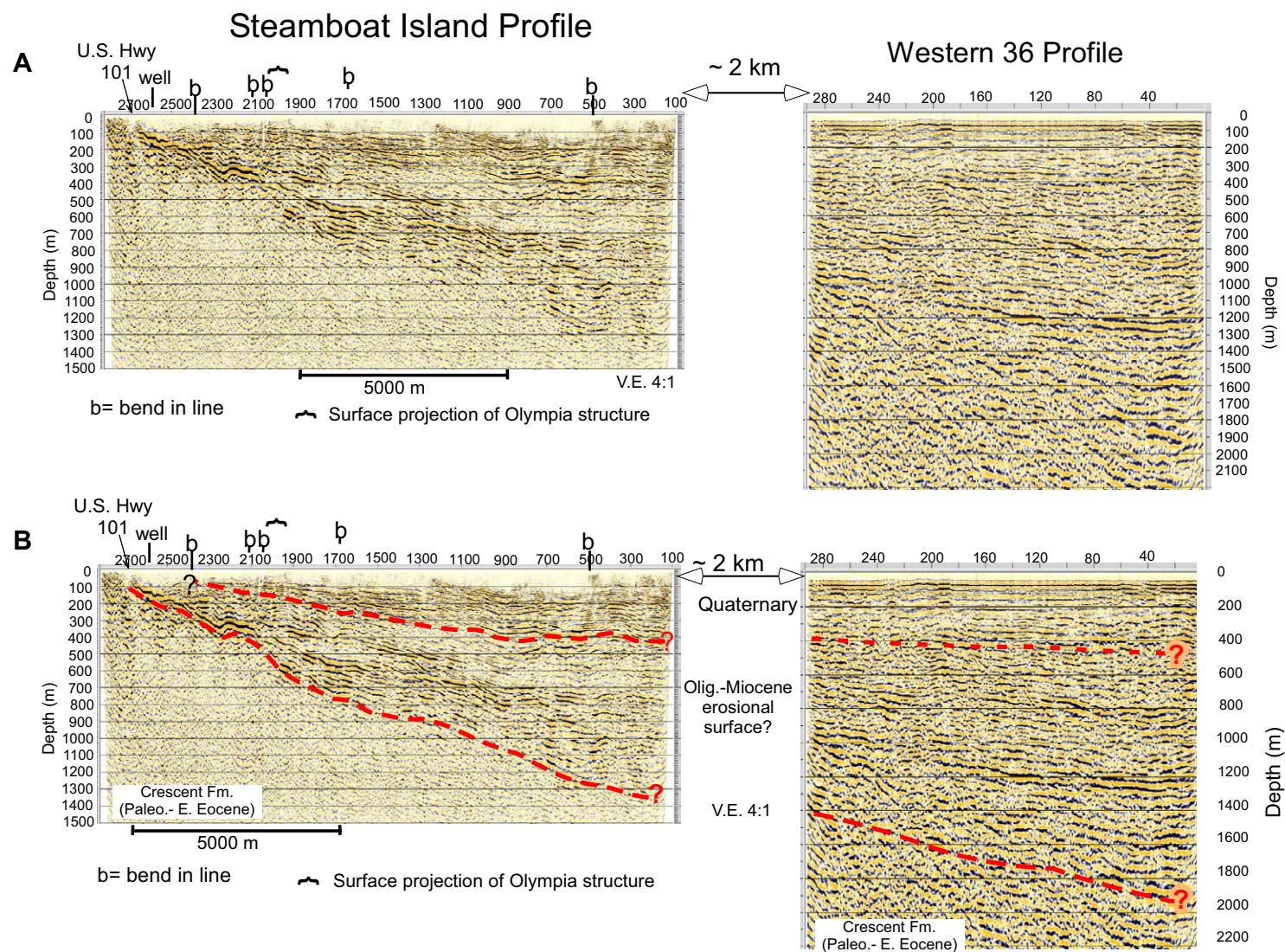


Figure 6. (A) Shown on the left is the migrated depth-converted 14.6-km-long Steamboat Island Road (SI) 144 channel land-based seismic reflection profile, which was acquired in 2010 using a mini-vibe source and 5 m geophone spacing. On the right is the 9-km-long Western 36, a single-channel industry marine profile (see Fig. 4 for location). V.E.—vertical exaggeration. (B) Migrated depth-converted seismic profiles showing an interpreted continuation of the gently dipping Crescent Formation surface in the southern Tacoma basin (Clement et al., 2010) to its outcrop in the Black Hills and onlapping Tertiary (i.e., Paleogene–Neogene) and Quaternary strata between a depth range of 0.1 and 1 km (Fig. 4).

The migrated, depth-converted seismic profiles reveal Eocene volcanic (Crescent Formation) rocks and onlapping Tertiary and Quaternary strata between depths of 0.1 and 1 km along the 14.6 km SI portion of the profiles (Fig. 6B). The imaged Crescent Formation surface has an apparent stratigraphic dip of $\sim 8^{\circ}$ – 10° . The upper part of the Crescent Formation consists of interbedded volcanic and sedimentary layers (Globberman et al., 1982; Babcock et al.,

1992). Due to an apparently low impedance contrast between the Paleocene to early Eocene volcanic and sedimentary rocks of the Crescent Formation and the overlying younger Tertiary sedimentary strata, it is difficult to clearly define the boundary that delineates the Crescent Formation bedrock surface (e.g., Johnson et al., 1994). In Pratt et al. (1997), discordance between gently north-dipping (2° – 4°) sedimentary strata in the southern Tacoma basin and

the underlying, more steeply dipping ($\sim 10^\circ$) reflectors that are interpreted to be Crescent Formation was used to tentatively delineate a basement surface on the Western 36 marine profile (Fig. 6B). Although the SI profile is higher resolution than the marine profile, low impedance contrasts between units make interpretation subjective. We define the top of the Crescent Formation on the SI profile as the zone where higher amplitude, fairly continuous reflectors (onlapping Tertiary strata) overlie relative nonreflective material. The interpreted Quaternary-Tertiary contact is placed where there appears to be a subtle difference in reflector character and overlying reflectors appear to be more horizontal. As shown in Figure 6B the surface separating the discordant strata on the Western 36 profile appears to project updip and correlate with our interpretation of the Crescent Formation surface on the north end of the SI seismic profile. The Crescent Formation is identified at a depth of ~ 75 m in a water well just north of Highway 101 (Logan and Walsh, 2004) and in exposures south of Highway 101 near the southern termination of the land-based profile (Figs. 4 and 6B). Reflector onlaps suggest that the Tertiary strata in the southern Tacoma basin were deposited on a sloping surface with only slight folding (2° – 4°) after deposition (e.g., Pratt et al., 1997). Other than the well on the left side of the profile near Highway 101 that reaches bedrock, there is little information available below surficial outcrops concerning the type, thickness, and age of the geologic materials along the SI profile. The geologic map of the Summit Lake 7.5 minute quadrangle, Thurston and Mason Counties (Washington State), covers approximately the southernmost third of the SI profile. Logan and Walsh (2004) stated “The contact between the Crescent Formation and sediments in the Puget Sound basin slopes moderately to steeply north-eastward (see cross section) so that in the northeast corner of this quadrangle, the basalt is overlain by a thick cover of Pleistocene glacial and nonglacial sediments, capped by late Wisconsinan-age Vashon Drift. For a discussion of the history of the Puget Lowland fill, see Walsh and others (2003).”

■ INTEGRATED GEOPHYSICAL DATA ANALYSIS

The geographical area of Figure 7A focuses on the portion of the magnetic anomaly map (Fig. 2B) that surrounds the marine (dashed and solid black lines) and SI seismic profiles (yellow line Figs. 2, 4, and 7A). On this anomaly map we overlay the magnetic boundary analysis lines (red) shown in Figure 3B with tick marks indicating direction toward higher amplitude magnetization. The projected surface location of the Olympia structure, as defined by the magnetic (heavy dots) and gravity (thick gray hachured) boundary analysis (Fig. 3E), is overlain on the magnetic anomaly map to show the location of the structure with respect to the seismic reflection profiles. Figure 7B is a graph of magnetic values extracted from the aeromagnetic data along the SI seismic profile with letters A–D being reference points along the graph and the SI seismic reflection profile (Fig. 7C). A colored box with dots above the graph and seismic profile indicate the location at which the trace of the Olympia structure defined by the magnetic boundary analysis gradient crosses the seismic

profile. Figure 7C shows our interpretation of faulting and deformation along the SI seismic profile. As observed on the marine seismic profiles P289–291, P292–294, and P300–301 (hachured bands in Figs. 3 and 4), a similar zone of deformation several kilometers wide is also observed near the north end of the SI profile (stations ~ 200 – 1300 , Fig. 7C). This deformation zone on the SI profile is characterized by small truncations and warped reflectors with small vertical displacements. Although we are confident that this zone of minor faulting is a continuation of deeper tectonic deformation, the lower resolution of the seismic profile with depth and the nonreflective character of the Crescent Formation prevent tracing the faults below the Crescent Formation surface.

■ DISCUSSION

Geophysical Anomaly Character of the Olympia Structure Trace

The question to be addressed is whether there is evidence to show that the location of the surface projection of the Olympia structure as defined by geophysical anomaly trends, at least within the confines of the study area, is predominantly constrained by observable tectonic deformation (faulting and/or folding). At a regional scale the Olympia structure is well defined by narrow and nearly linear aeromagnetic and gravity anomalies coincident with the north-east flank of the Black Hills uplift (Figs. 1B, 1C, and 2A). Boundary analysis of regional aeromagnetic and gravity anomaly data sets (Figs. 3A–3E) reveals that although the overall anomaly traces of the Olympia structure visually match the regional trend closely, the traces are in actuality a composite of discontinuous anomalies that at local scale are complexly oriented. Magnetic boundary analysis provides gradient lines (red in Figs. 3B and 7A) that define geologic units of varying physical properties (i.e., lithologic composition of varying magnetic intensity and polarity) within the Crescent Formation volcanic assemblage. In map view, bedrock areas with strong magnetic gradients caused by abrupt variations in magnetization intensity and/or polarity define the magnetic anomaly trace of the Olympia structure. These magnetic boundaries are highlighted with a heavy black dot pattern, whereas the trace of the Olympia structure defined by gravity boundary analysis lines is shown as a gray hachured band (Fig. 7A). The magnetic anomaly map and magnetic value graph (Figs. 7A, 7B) show that the steepest gradient, indicating the most dramatic change in bedrock magnetism, that corresponds to the trace of the Olympia structure, is approximately midway between reference points A and B. One explanation for this steep magnetic gradient is that it results from a combination of normally magnetized Crescent Formation basement rock being uplifted by thrust or reverse faulting (north of reference point A) and placed next to a pronounced low magnetic trough (south of reference point B) formed by normal faulted or downwarped Crescent Formation that is infilled with weakly magnetic to nonmagnetic Tertiary sediment. This tectonic scenario would suggest that the Olympia structure trace is controlled by thrust and/or normal faulting with displaced bedrock juxtaposed against a thick section of Tertiary deposits.

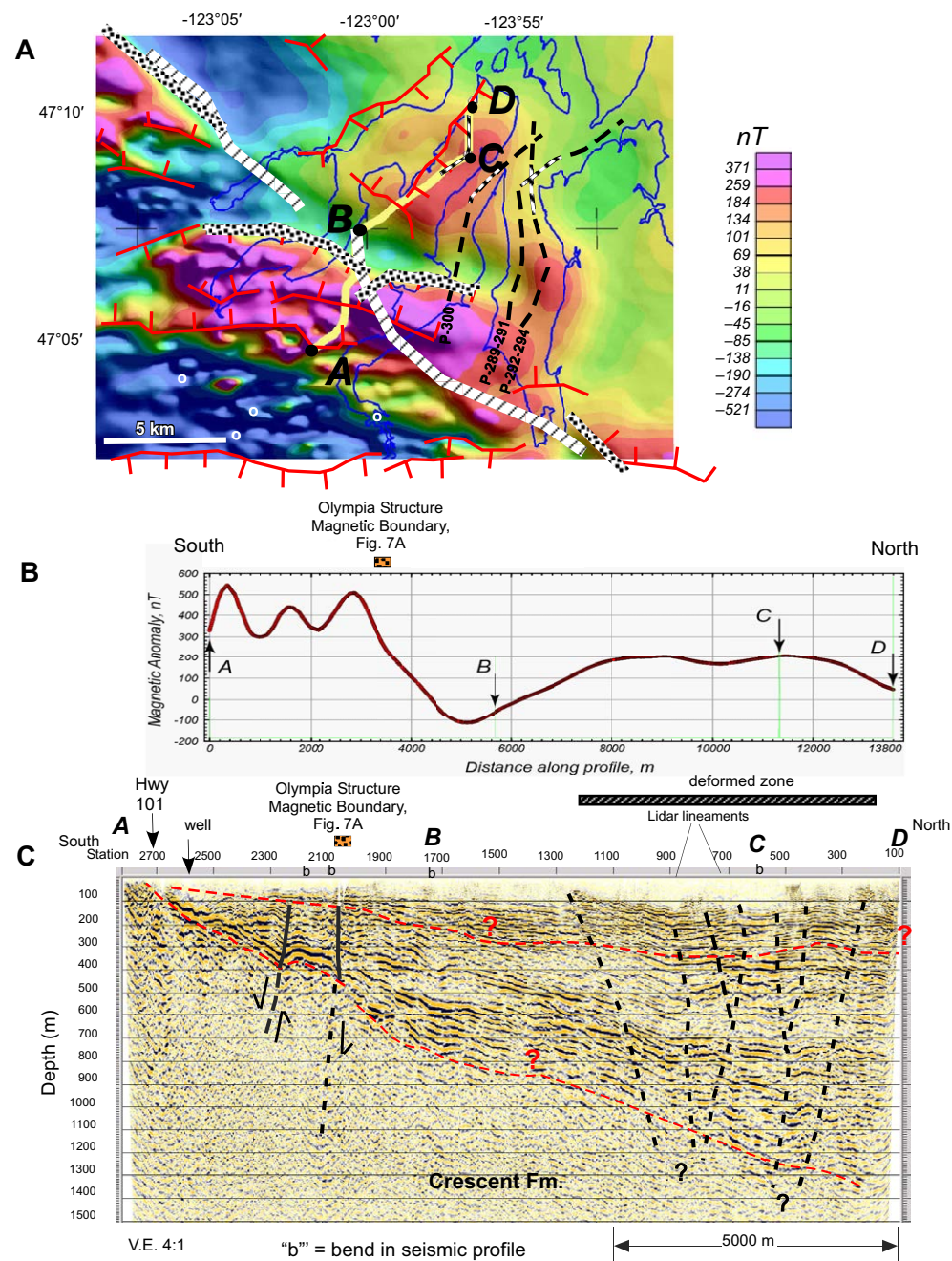


Figure 7. (A) Magnetic anomaly base map (Fig. 2B). Barbed red lines are magnetic gradient boundaries derived from boundary analysis (Fig. 3B); barbs are in the direction of higher magnetic value rock. Surface location of Olympia structure defined by gravity (thick gray hatched line) and magnetic (thick black dotted line) anomaly boundary analysis (Fig. 3E). White circles in southwest quadrant indicate locations where rocks are reversely magnetized (Globberman et al., 1982). The yellow line represents the location of the Steamboat Island Road (SI) seismic reflection profile with respect to the magnetic anomalies base map. Reference point letters A–D along the yellow seismic reflection line correlate with the same letters on the magnetic value graph (Fig. 7B) and along the interpreted SI seismic reflection profile in C. (B) Graph showing variation in magnetic values extracted from aeromagnetic anomalies (Fig. 2C) along the SI seismic reflection profile (Fig. 7C). Colored dotted box above magnetic value graph (B) and interpreted SI seismic profile (C) indicate the location where the Olympia structure crosses the (SI) seismic reflection profile on the magnetic anomalies base map. (C) Interpreted SI seismic reflection profile. Hatched black and white bands on seismic profile location lines (Figs. 4 and 7A) represent zones with varying degrees of deformation observed on all seismic profiles (Clement et al., 2010, and this study). Lidar—light detection and ranging; VE—vertical exaggeration.

Seismic Reflection Expression of the Olympia Structure

The primary result of the seismic reflection profiling is that the Olympia structure does not correspond with a thrust fault causing substantial displacement of Tertiary strata deposited on the Crescent Formation rocks. The ~26-km-long interpreted seismic reflection profiles (Figs. 4 and 6) image the Crescent Formation bedrock surface from where it crops out in the Black Hills just south of the land-based SI profile to ~2 km depth at the northeast end of the Western 36 marine profile. With only minor variations along the seismic reflection profiles (Fig. 6) the interpreted Crescent Formation bedrock surface has a relatively consistent northeast dip of ~10° (note the 4:1 vertical exaggeration on the seismic reflection profile; Figs. 6 and 7C). Only the 14.6-km-long SI land-based seismic reflection profile crosses the geophysically defined trace of the Olympia structure.

Near stations 2250 and 2050, on the south end of the SI profile, a pair of faults appears to uplift a small block of bedrock. Although the differentiation of the Crescent Formation surface from overlying Tertiary rock is unclear beneath the thick sediment on the Western 36 profile, the contact is well defined on the SI profile, and it is believed that maximum south side up displacement on the fault at station 2050 is no more than 100 m. This slightly uplifted block corresponds with the north edge of the magnetic high values (purple area north of reference point A; Figs. 7A, 7B), and the fault at station 2050 correlates with the location of the median of the magnetic gradient that defines the trace of the Olympia structure (Fig. 7A). However, evidence for the amount of bedrock surface displacement and accompanied sediment thickening needed to change the magnetic value by nearly 500 nT over a short distance is not supported by faulting and bedrock offset of the Crescent Formation imaged on the SI seismic reflection profile (Fig. 7C). An additional example illustrating that increasing Tertiary and Quaternary sediment thickening plays only a minor, if any, role in the observed magnetic value is seen on the northeast end of the seismic profile between reference points B and D. The anomaly map and magnetic profile (Figs. 7A, 7B) show that the traverse along the seismic reflection profile northeast from reference point B to near the end of the profile crosses a relatively broad positive value, normally magnetized, anomaly as the seismic reflection profile (Figs. 6 and 7C) shows increasing Tertiary sediment thickening over a deepening Crescent Formation surface.

Reversed Crescent Formation Magnetic Polarity and the Olympia Structure

An alternative explanation for the magnetic anomaly patterns and abrupt variation in bedrock magnetic values is that the magnetic anomaly patterns reflect rock physical property variations such as reversed magnetization rather than major tectonic faulting and vertical offset of the Crescent Formation bedrock surface. White circles within the dark blue patterned magnetic anomaly in the lower left corner of Figure 7A are locations of reversely magnetized basalt units measured by Globerman et al. (1982) in the Summit Lake quadrangle in

which the south end of the SI profile terminates. The Sheldon Valley quadrangle, ~10 km to the northwest of the Summit Lake quadrangle (Logan and Walsh, 2004), has a similar geologic arrangement, where exposed Crescent Formation basaltic rocks along the northwest-trending Black Hills flank are overlapped by Tertiary and Quaternary sediments. Preliminary mapping indicates that the distribution of aeromagnetic highs and lows with respect to the distribution of basalt exposures leaves little doubt that some of the Sheldon Valley basalt is reversely magnetized, like exposed basalts in the Summit Lake quadrangle just south of the SI seismic profile (M. Polenz, 2016, personal commun.).

S. Magsino (2016, personal commun.) provided the following assessment of unpublished modeling of aeromagnetic and ground magnetic data sets along trend of the SI profile. (1) Given that models provide nonunique geologic scenario solutions, it was determined that displacements of Tertiary sediments were not necessary and that the steep gradient, localized anomalies in the higher resolution ground magnetic data, not seen by the aeromagnetic data, seem to be controlled by contacts between normally and reversely magnetized Crescent Formation units. (2) Thickness estimates of either normal or reversed individual volcanic units are not obtainable from the data sets and have been equally difficult to determine by mapping. (3) Modeling showed that varying numbers of southwest-directed thrust faults, compatible with the north-south compressive regime, could stack varying thicknesses of normal and reversed units to account for different magnetic anomaly intensities along strike of the model and the seismic profile. (4) The occurrence of Holocene activity on inferred faults could not be determined.

Figure 8 shows one possible model for the Olympia structure, based on aeromagnetic and isostatic residual gravity anomalies and constrained by seismic reflection data. Models based on potential-field data are nonunique; i.e., an infinite variety of models can be derived that mathematically fit observed gravity and magnetic data. The intent of this particular model (Fig. 8) is to show that the complexity of magnetic anomalies over the Olympia structure can be explained regardless of the lack of topography on the top surface of Crescent Formation. The guiding principle behind Figure 8 was to maintain the monoclinical nature of the contact between Crescent Formation and overlying sediments, as deduced from seismic reflection data (Fig. 7C), using induced and remanent magnetization contrasts within the Crescent Formation to explain short-wavelength, high-amplitude magnetic anomalies. In Figure 8, we assumed that magnetization contrasts in the Crescent are caused by folded and faulted contacts between normal and reversely magnetized Crescent Formation strata. Other explanations are possible, including contacts between upper- and lower-member Crescent Formation basalts, as modeled in the Olympic Peninsula by Blakely et al. (2009).

If the major magnetic anomalies are caused by reversals in the magnetic properties of the basalt units, it raises the possibility that these units are juxtaposed by faults with substantial displacements. The lack of coherent reflectors below the top of the Crescent Formation bedrock interface imaged on the seismic profiles means that faults could be present and escape notice in the data, if they do not substantially displace the upper surface of the Crescent Formation

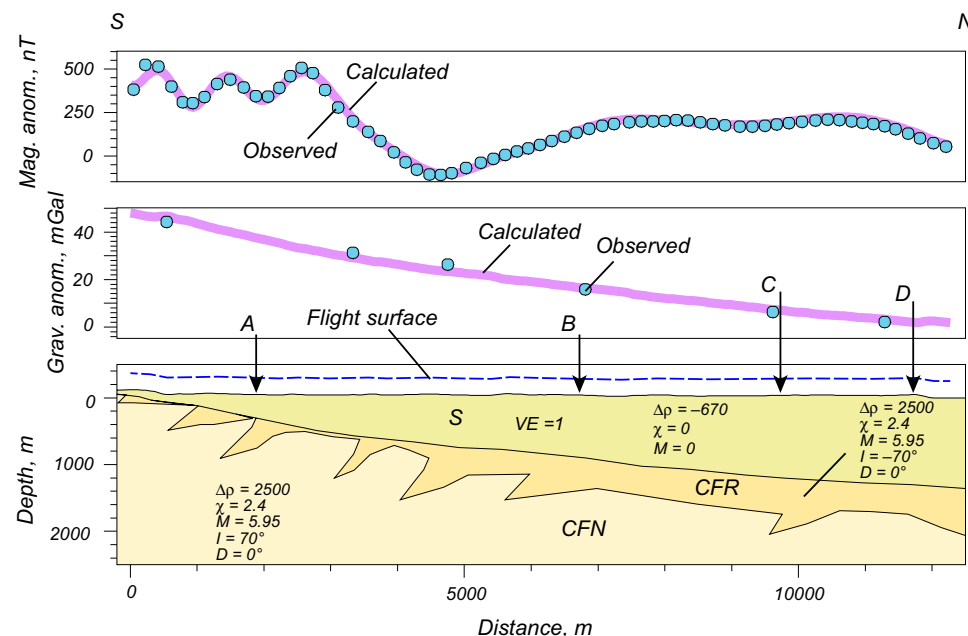


Figure 8. Cross-sectional model of the Olympia structure based on aeromagnetic and isostatic residual gravity anomalies and constrained by seismic reflection data. Gravity and magnetic contacts are assumed uniform and infinitely extended in the direction perpendicular to the profile. The contact between the Crescent Formation and overlying sediment is constrained by the seismic reflection image shown in Figure 7C. (See Fig. 7A for locations of labels A–D.) S—post-Eocene sediments; CFN—normally magnetized Crescent Formation; CFR—reversely magnetized Crescent Formation; $\Delta\rho$ is the bulk density relative to crustal standard (2670 kg/m³); χ is the magnetic susceptibility in SI units, multiplied by 1000; M is the intensity of remnant magnetization in A/m; I is remnant inclination; D is remnant declination. Remnant magnetization intensity and magnetic susceptibility values are from Finn (1990) and Blakely et al. (2009).

rocks or the overlying Tertiary sedimentary strata. Thus, pre-Tertiary faults with large displacement may have contributed to the uplift of the Black Hills, so long as post-Tertiary motion is relatively small (<~100 m).

Shallow Faulting and Deformation

Zones of deformed sedimentary strata observed on the marine surveys (Figs. 4, 5, and 7A) are found several kilometers north of the projected location of the Olympia structure (Fig. 4). Clement et al. (2010) described high-resolution, single-channel, shallow (<100 m depth) marine profiles that show the zones of deformation as having minor faults cutting subglacial or postglacial strata of late Pleistocene or Holocene age. These interpreted faults show opposite senses of displacement on reflectors at different depths, and relatively small vertical displacements. Although these faults are within the zones of deformed reflectors on all three Budd and Eld Inlet marine profiles, individual faults cannot be correlated between the widely spaced profiles because of changes in strata and fault character. However, Clement et al. (2010) noted that if the faults interpreted on the marine profiles were linked, their general trend would be toward two faint Lidar (light detection and ranging) lineaments that have been identified on the Steamboat Island peninsula (Figs. 4 and 7C). Field inspection of these Lidar lineaments shows only slight elevation changes, and they would not normally be identified as a fault scarp (B. Sherrod, 2012, personal commun.). Clement et al.

(2010) argued that the faults seen in the marine seismic profiles are tectonic in origin rather than being due to glacial processes, and speculated that if the faults are shallowly rooted they may be bending-moment faults accommodating deeper folding. Alternatively, they may be splay to structures that have larger basement displacement located farther to the south. Clement et al. (2010) also suggested that these faults are part of a strike-slip fault system because of the lack of evidence for thrust faulting on deeper strata, the vertical attitude of the faults, and the variability of reflector vertical displacements at different depths.

Similar to the ~2-km-wide zone of deformed reflectors and faulting just described there is a zone of faulted and deformed reflectors between stations 200 and 1300 on the north end of the SI seismic reflection profile. These faulted and deformed reflectors are primarily visible within the Tertiary and Quaternary section to the shallowest resolved reflector at ~75 m depth (Fig. 7C). These faults must originate from deeper structures within the Crescent Formation; however, a potentially low impedance contrast between the Tertiary and Crescent Formation boundary and the nonreflective character of strata within the Crescent Formation do not provide clear evidence of fault traces below the Crescent Formation surface. The SI profile crosses the two weak Lidar lineaments at approximately stations 700 and 900 (Figs. 4 and 7C). Although the lineaments are within the zone of deformed Tertiary and Quaternary reflectors, and faults are interpreted to cut shallow reflectors beneath the lineament traces, whether the lineaments can be interpreted as fault scarps is unclear. The deformed strata

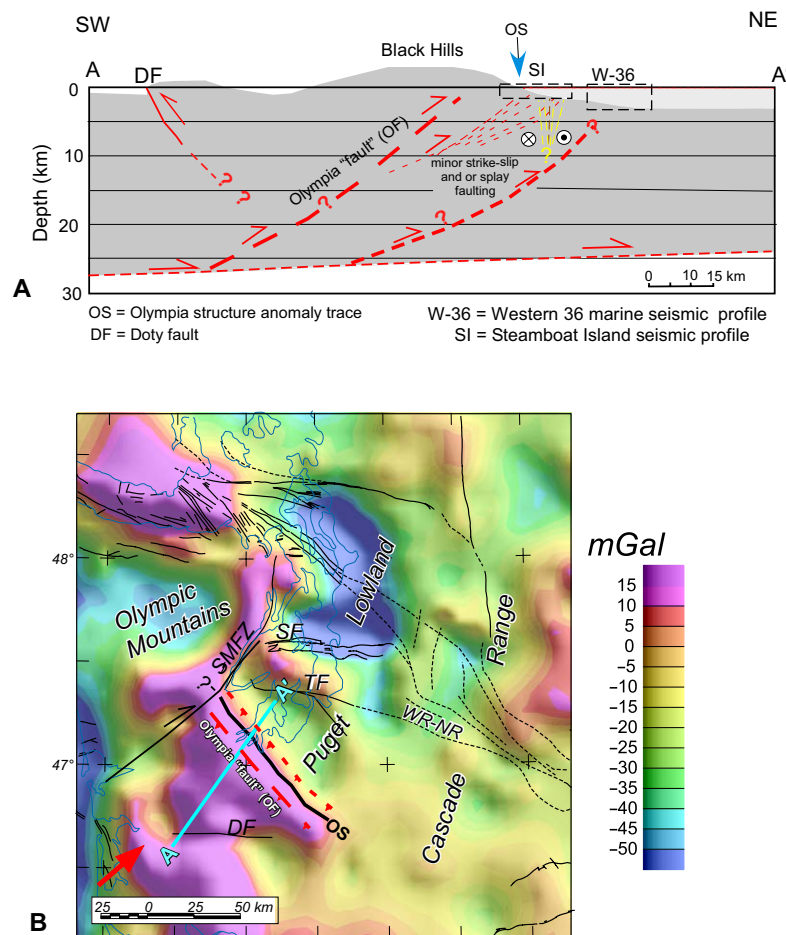


Figure 9. (A) Cross section showing a hypothetical model arrangement of tectonic features associated with the Black Hills structural uplift; see text discussion for explanation. Note the shallow and limited areal extent of high-resolution seismic reflection imaging (SI, W-36) and associated geophysical analysis with respect to the overall area of the Black Hills tectonic structures. Thin yellow (strike slip) and red lines (thrust splay) represent possible origins for minor faults observed on the seismic reflection profiles. (B) Regional isostatic residual gravity anomaly base map showing location of hypothetical cross section A-A' (modified from Blakely et al., 2009). Black line labeled OS is location of Olympia structure, most often cited in literature as the Olympia fault. Large dashed red line represents a plausible location for a yet to be identified Olympia blind thrust faults responsible for the fault bend fold Black Hills uplift. Small dashed line represents a possible location for another blind thrust northeast of the OS. Solid and dashed black lines represent interpreted connections between the Yakama fold and thrust belt and Puget Lowland faults (Blakely et al., 2011). Red arrow indicates direction of regional compression. TF—Tacoma fault; WR-NR—White River–Naches River faults; SMFZ—Saddle Mountain fault zone (Blakely et al., 2009, 2011); SF—Seattle fault zone; other abbreviations as in A.

and minor faulting in zones on the SI and marine profiles are in similar geographic locations, as shown by the hachured polygon box in Figure 4. The overall orientation of the zone of shallow reflector disruption shown in Figure 4 is slightly northwest to east-west; however, the orientations of the individual faults encompassed by the zone are unknown. Without clear evidence of strike direction for faults within any of the deformation zones it is impossible to determine continuity of faults between profiles, and the overall style of faulting. Geologic mapping of the basalt flows in both the Summit Lake quadrangle south of the SI profile and in preliminary mapping in the Sheldon Valley quadrangle have identified northeast-striking lineaments and multiple orientations of shearing in bedrock and Quaternary sediments (M. Polenz, 2016, personal commun.). It is unknown if there is a tectonic relationship between mapped lineaments and shear zones in the discontinuous Crescent Formation units and the deformed and faulted sediments interpreted on the seismic reflection profiles.

Based on the faulting characteristics seen on the SI profile between stations 200 and 1300 (Fig. 7C), we speculate that the faults may be related to a wide zone of anastomosing oblique strike-slip fault segments or shallow-rooted tension faulting related to underlying thrust faults. Although the faults farther south appear to have a different character on the seismic reflection profile, it is unknown if they are part of a wider zone of deformation or if they are related to a different style of tectonics. Wells and Coe (1985) and Stanley et al. (1996) suggested that (1) uplift and folding of discrete basement blocks, including the Black Hills, began during the middle to late Eocene; and (2) that some block-bounding faults have evolved through the Tertiary into oblique strike-slip fault systems to accommodate both regional north-south transpression and documented clockwise rotation.

Cross-section A-A' in Figure 9A shows a hypothetical arrangement of tectonic features associated with the Black Hills structural uplift and suggests that multiple tectonic styles, minor splay thrust faults, and/or a zone of strike-slip faulting, could be responsible for the faulting and deformation seen on the seismic reflection profiles. Note the shallow and limited areal extent of high-resolution seismic reflection imaging (SI and W-36) and associated geophysical analysis with respect to the overall area of the Black Hills tectonic structures. Figure 9B shows the relationship of the Black Hills uplift with respect to other fault systems in the Puget Lowland. Based on currently available geophysical data sets, we suggest that the geophysically defined anomaly trace of the Olympia structure (OS black line in Fig. 9B) should be considered an anomaly trend and that the yet to be identified Olympia fault (or faults; red OF in Fig. 9B) responsible for the probable fault bend fold Black Hills uplift is somewhere to south in the core of the uplift.

SUMMARY

Figure 9A shows a hypothetical cross section of the Black Hills uplift and Tacoma basin. The SI and marine Western 36 seismic profiles (dashed black boxes) and accompanying anomaly map and profiles image only a shallow

section of the gently dipping northeast flank of the Black Hills uplift. Based on the available local high-resolution seismic reflection and geophysical anomaly data sets that cross the anomaly defined surface projection of the Olympia structure, we find no clear evidence in our data to support the interpretation of a basement-displacing fault or faults and abrupt thickening of the sedimentary sections at the trace location. As an alternative we suggest that an arrangement of juxtaposed normal and reversed magnetized volcanic units can create the strong magnetic anomaly gradient boundaries that define the Olympia structure trace through our study area. However, due to the logistically constrained shallow nature of the available geophysical data sets, as is evident by the dashed rectangle boxes indicating the location of the seismic profiles on northeast flank of the Black Hills (Fig. 9A), we cannot discount that deeper mid-crustal structures exist. The zone of strata deformation and faulting observed on the marine profiles, and better imaged on the land-based seismic profile, indicate that a source of tectonic deformation is active several kilometers north of the Olympia structure trace. Due to the lack of orientation information and the inability to identify a faulting style, we speculate that the deformation and faulting observed on the seismic profiles, and possibly in geologic mapping, are the shallow representation of a deeper system of north-south regional compression-induced strike-slip faulting. The Figure 9A cross section and Figure 9B map view also suggest that the Black Hills is a fault-propagation fold above an as yet to be identified blind thrust fault system buried beneath the core of the Black Hills. We suggest that until there are additional geophysical surveys and geologic mapping across the Olympia structure, this enigmatic feature should be considered a geophysically defined structure rather than a fault.

ACKNOWLEDGMENTS

This work was supported by the Earthquake Hazards Program of the U.S. Geological Survey. We thank Z. Maharrey, R. Dart, C. Volpi, B. King, and M. Conley for their assistance in acquiring the Steamboat Island Road seismic reflection profile. We also thank the University of Texas NEES (George E. Brown, Jr. Network for Earthquake Engineering Simulation) for providing the minivibe source and C. Hoffpauir (minivibe operator). Reviews by Brian Sherrod, Megan Anderson, and Thomas Brocher strengthened and added focus to this paper. We also benefited from many discussions with colleagues M. Polenz and T. Walsh (Washington Department of Natural Resources, Division of Geology and Earth Resources). We thank S. Magsino, who graciously contributed insight, comments, and preliminary models from her work on the southern Puget Lowland. Any use of trade, product, or firm names is for descriptive purposes only, and does not imply endorsement by the U.S. Government.

REFERENCES CITED

- Atwater, T., 1970, Implications of plate tectonics for the Cenozoic evolution of western North America: *Geological Society of America Bulletin*, v. 81, p. 3513–3536, doi:10.1130/0016-7606(1970)81[3513:IOPTFT]2.0.CO;2.
- Atwater, B.F., and Moore, A.L., 1992, A tsunami about 1000 years ago in Puget Sound, Washington: *Science*, v. 258, p. 1614–1617, doi:10.1126/science.258.5088.1614.
- Babcock, R.S., Burmester, R.F., Engebretson, D.C., Warnock, A., and Clark, K.P., 1992, A rifted margin origin for the Crescent basalts and related rocks in the northern Coast Range volcanic province, Washington and British Columbia: *Journal of Geophysical Research*, v. 97, p. 6799–6821, doi:10.1029/91JB02926.

- Barnett, E.A., Sherrod, B.L., Hughes, J.F., Kelsey, J.L., Walsh, T.J., Contreras, T.A., Schermer, E.R., and Carson, R.J., 2015, Paleoseismic evidence for late Holocene tectonic deformation along the Saddle Mountain fault zone, southeastern Olympic peninsula, Washington: *Seismological Society of America Bulletin*, v. 105, p. 38–71, doi:10.1785/0120140086.
- Blakely, R.J., 1995, *Potential theory in gravity and magnetic applications*: New York, Cambridge University Press, 441 p., doi:10.1017/CBO9780511549816.
- Blakely, R.J., and Simpson, R.W., 1986, Approximating edges of source bodies from magnetic and gravity anomalies: *Geophysics*, v. 51, p. 1494–1498, doi:10.1190/1.1442197.
- Blakely, R.J., Wells, R.E., and Weaver, C.S., 1999, Puget Sound aeromagnetic maps and data: U.S. Geological Survey Open-File Report 99-514, pubs.usgs.gov/of/1999/of99-514/.
- Blakely, R.J., Wells, R.E., Weaver, C.S., and Johnson, S.Y., 2002, Location, structure, and seismicity of the Seattle fault zone, Washington: Evidence from aeromagnetic anomalies, geologic mapping, and seismic-reflection data: *Geological Society of America Bulletin*, v. 114, p. 169–177, doi:10.1130/0016-7606(2002)114<0169:LSASOT>2.0.CO;2.
- Blakely, R.J., Sherrod, B.L., Hughes, J.F., Anderson, M.L., Wells, R.E., and Weaver, C.S., 2009, Saddle Mountain fault deformation zone, Olympic Peninsula, Washington: Western boundary of the Seattle uplift: *Geosphere*, v. 5, p. 105–125, doi:10.1130/GES00196.1.
- Blakely, R.J., Sherrod, B.L., Weaver, C.S., Wells, R.E., Rohay, A.C., Barnett, E.A., and Knepprath, N.E., 2011, Connecting the Yakima fold and thrust belt to active faults in the Puget Lowland, Washington: *Journal of Geophysical Research*, v. 116, B07105, doi:10.1029/2010JB008091.
- Booth, D.B., Troost, K.G., Clague, J.J., and Waitt, R.B., 2004, The Cordilleran ice sheet, in Gillespie, A.R., et al., eds., *The Quaternary Period in the United States: Developments in Quaternary Science 1*: Amsterdam, Netherlands, Elsevier Press, p. 17–43, doi:10.1016/S1571-0866(03)01002-9.
- Brocher, T.M., Parsons, T., Blakely, R.J., Christensen, N.I., Fisher, M.A., and Wells, R.E., 2001, Upper crustal structure in Puget lowland, Washington: Results from the 1998 seismic hazards investigation on Puget Sound: *Journal of Geophysical Research*, v. 106, p. 13,541–13,564, doi:10.1029/2001JB000154.
- Brocher, T.M., Blakely, R.J., and Wells, R.E., 2004, Reinterpretation of the Seattle Uplift, Washington, as a passive roof duplex: *Seismological Society of America Bulletin*, v. 94, p. 1379–1401.
- Bucknam, R.C., Hemphill-Haley, E., and Leopold, E.B., 1992, Abrupt uplift within the past 1700 years at southern Puget Sound, Washington: *Science*, v. 258, no. 5088, p. 1611–1614, doi:10.1126/science.258.5088.1611.
- Clement, C.R., Pratt, T.L., Holmes, M.L., and Sherrod, B.L., 2010, High-resolution reflection imaging of growth folding and faults beneath the southern Puget lowland: Washington State: *Seismological Society of America Bulletin*, v. 100, p. 1710–1723, doi:10.1785/0120080306.
- Daneš, Z.F., Bonno, M.M., Brau, E., Gilham, W.D., Hoffman, T.F., Johnansen, D., Jones, M.H., Malfait, B., Masten, J., and Teague, G.O., 1965, Geophysical investigation of the southern Puget Sound Area, Washington: *Journal of Geophysical Research*, v. 70, p. 5573–5580, doi:10.1029/JZ070i022p05573.
- DeMets, D., Gorden, R.G., Argus, D.F., and Stein, S., 1994, Effect of recent revisions to the geomagnetic reversal time scale on estimates of current plate motions: *Geophysical Research Letters*, v. 21, p. 2191–2194, doi:10.1029/94GL02118.
- Finn, C.W., 1990, Geophysical constraints on Washington convergent margin structure: *Journal of Geophysical Research*, v. 95, p. 19,533–19,546, doi:10.1029/JB095iB12p19533.
- Finn, C.W., Philips, M., and Williams, D.L., 1991, Gravity anomaly and terrain maps of Washington: U.S. Geological Survey Geophysics Investigation Map GP-988.
- Globerman, B.R., Beck, M.E., and Duncan, R.A., 1982, Paleomagnetism and tectonic significance of Eocene basalts from the Black Hills, Washington Coast Range: *Geological Society of America Bulletin*, v. 93, p. 1151–1159, doi:10.1130/0016-7606(1982)93<1151:PATSOE>2.0.CO;2.
- Gower, H.D., Yount, J.C., and Crosson, R.S., 1985, Seismotectonic map of the Puget Sound region, Washington: U.S. Geological Survey Miscellaneous Investigation Series Map I-1613, 15 p., scale 1:250,000.
- Johnson, S.Y., Potter, C.J., and Armentrout, J.M., 1994, Origin and evolution of the Seattle fault and Seattle basin, Washington: *Geology*, v. 22, p. 71–74, doi:10.1130/0091-7613(1994)022<0071:OAEOTS>2.3.CO;2.
- Johnson, S.Y., Dadisman, S.V., Childs, J.R., and Stanley, W.D., 1999, Active tectonics of the Seattle fault and central Puget Sound, Washington: Implications for earthquake hazards: *Geological Society of America Bulletin*, v. 111, p. 1042–1053, doi:10.1130/0016-7606(1999)111<1042:ATOTSF>2.3.CO;2.

- Johnson, S.Y., Blakely, R.J., Stephenson, W.J., Dadisman, S.V., and Fischer, M.A., 2004, Active shortening of the Cascadia forearc and implications for seismic hazards of the Puget Lowland: *Tectonics*, v. 23, TC1011, doi:10.1029/2003TC001507.
- Kelsey, H.M., Sherrod, B.L., Johnson, S.Y., and Dadisman, S.V., 2004, Land-level changes from late Holocene earthquakes in the northern Puget Lowland, Washington: *Geology*, v. 32, p. 469–472, doi:10.1130/G20361.1.
- Kelsey, H.M., Sherrod, B.L., Nelson, A.R., and Brocher, T.M., 2008, Earthquakes generated from bedding plane-parallel reverse faults above an active wedge thrust, Seattle fault zone: *Geological Society of America Bulletin*, v. 120, p. 1581–1597, doi:10.1130/B26282.1.
- Lamb, A.P., Liberty, L.M., Blakely, R.J., Pratt, T.L., Sherrod, B.L., and van Wijk, K., 2012, Western limits to the Seattle fault zone and its interaction with the Olympic Peninsula, Washington: *Journal of Geophysical Research*, v. 117, B03105, doi:10.1029/2011JB008722.
- Lees, J.M., and Crosson, R.S., 1990, Tomographic imaging of local earthquake delay times for 3-D velocity variation in western Washington: *Journal of Geophysical Research*, v. 95, p. 4763–4776, doi:10.1029/JB095iB04p04763.
- Liberty, L.M., and Pratt, T.L., 2008, Structure of the eastern Seattle fault zone, Washington State: New insights from seismic reflection data: *Seismological Society of America Bulletin*, v. 98, p. 1681–1695, doi:10.1785/0120070145.
- Logan, R.L., and Walsh, T.J., 2004, Geology map of the Summit Lake 7.5 minute quadrangle, Thurston and Mason Counties, Washington: Washington Division of Geology and Earth Resources Open-File Report 2004-10, scale 1:24,000.
- Mace, C.G., and Keranen, K.M., 2012, Oblique fault systems crossing the Seattle basin: Geophysical evidence for additional shallow fault systems in the central Puget Lowlands: *Journal of Geophysical Research*, v. 117, B03105, doi:10.1029/2011JB008722.
- Magsino, S., Sanger, E., Walsh, T.J., Palmer, S.P., and Blakely, R.J., 2003, The Olympia structure: Ramp or discontinuity? New gravity data provide more information: *Geological Society of America Abstracts with Programs*, v. 35, no. 6, p. 479.
- Mazzotti, S., Dragert, H., Hyndman, R.D., Miller, M.M., and Henton, J.A., 2002, GPS deformation in a region of high crustal seismicity: N. Cascadia forearc: *Earth and Planetary Science Letters*, v. 198, p. 41–48, doi:10.1016/S0012-821X(02)00520-4.
- McCaffrey, R., Qamar, A.I., King, R.W., Wells, R., Khazaradze, G., Williams, C.A., Stevens, C.W., Vollick, J.J., and Zwick, P.C., 2007, Fault locking, block rotation and crustal deformation in the Pacific Northwest: *Geophysical Journal International*, v. 169, p. 1315–1340, doi:10.1111/j.1365-246X.2007.03371.x.
- McCaffrey, R., King, R., Payne, S.J., and Lancaster, M., 2013, Active tectonics of northwestern U.S. inferred from GPS-derived surface velocities: *Journal of Geophysical Research*, v. 118, p. 1–5, doi:10.1029/2012JB009473.
- Nelson, A.R., Johnson, S.Y., Kelsey, H.M., Wells, R.E., Sherrod, B.L., Pezzopane, S.K., Bradley, L.A., Koehler, R.D., and Bucknam, R.C., 2003, Late Holocene earthquakes on the Toe Jam Hill fault, Seattle fault zone, Bainbridge Island, Washington: *Geological Society of America Bulletin*, v. 115, p. 1388–1403, doi:10.1130/B25262.1.
- Nelson, A.R., Kelsey, H.M., and Witter, R.C., 2006, Great earthquakes of variable magnitude at the Cascadia subduction zone: *Quaternary Research*, v. 65, p. 354–365, doi:10.1016/j.yqres.2006.02.009.
- Nelson, A.R., Personius, S.F., Sherrod, B.L., Kelsey, H.M., Johnson, S.Y., Bradley, L.A., and Wells, R.E., 2014, Diverse rupture modes for surface-deforming upper plate earthquakes in the southern Puget Lowland of Washington State: *Geosphere*, v. 10, p. 769–796, doi:10.1130/GES00967.1.
- Petersen, M.D., Cramer, C.H., and Frankel, A.D., 2002, Simulations of seismic hazards for the Pacific Northwest of the United States from earthquakes associated with the Cascadia subduction zone: *Pure and Applied Geophysics*, v. 159, p. 2147–2168, doi:10.1007/s00024-002-8728-5.
- Phillips, J.D., Hansen, R.O., and Blakely, R.J., 2007, The use of curvature in potential-field interpretation: *Exploration Geophysics*, v. 38, p. 111–119, doi:10.1071/EG07014.
- Pratt, T.L., Johnson, S.Y., Potter, C., Stephenson, W.J., and Finn, C.W., 1997, Seismic-reflection images beneath Puget Sound, western Washington State: The Puget Lowlands thrust sheet hypothesis: *Journal of Geophysical Research*, v. 102, p. 27,469–27,489, doi:10.1029/97JB01830.
- Pratt, T.L., Troost, K.G., Odum, J.K., and Stephenson, W.J., 2015, Kinematics of shallow back-thrusts in the Seattle fault zone, Washington State: *Geosphere*, v. 11, p. 1948–1974, doi:10.1130/GES01179.1.
- Schuster, J.E., 2005, Geologic map of Washington state: Washington, Division of Geology and Earth Resources Geologic Map GM-53, scale 1:250,000.
- Sherrod, B.L., 2001, Evidence for earthquake-induced subsidence about 1100 yr ago in coastal marshes of southern Puget Sound, Washington: *Geological Society of America Bulletin*, v. 113, p. 1299–1311, doi:10.1130/0016-7606(2001)113<1299:EFEISA>2.0.CO;2.
- Sherrod, B.L., Buckman, R.C., and Leopold, E.B., 2000, Holocene relative sea level changes along the Seattle fault at Restoration Point, Washington: *Quaternary Research*, v. 54, p. 384–393, doi:10.1006/qres.2000.2180.
- Sherrod, B.L., Brocher, T.M., Weaver, C.S., Buckman, R.C., Blakely, R.J., Kelsey, H.M., Nelson, A.R., and Haugerud, R.A., 2004, Holocene fault scarps near Tacoma, Washington: *Geology*, v. 32, p. 9–12, doi:10.1130/G19914.1.
- Simpson, R.W., Jachens, R.C., Blakely, R.J., and Saltus, R.W., 1986, A new isostatic residual gravity map of the conterminous United States with a discussion of the significance of isostatic residual anomalies: *Journal of Geophysical Research*, v. 91, p. 8348–8372, doi:10.1029/JB091iB08p08348.
- Snively, P.D., Jr., and Wells, R., 1996, Cenozoic evolution of the continental margin of Oregon and Washington, in Roger, A.M., et al., eds., *Assessing Earthquake Hazards and Reducing Risk in the Pacific Northwest*: U.S. Geological Survey Professional Paper 1560, p. 161–182.
- Stanley, W.D., Johnson, S.Y., and Nuccio, V.F., 1994, Analysis of Deep Seismic-Reflection and Other Data from the Southern Washington Cascades: U.S. Geological Survey Open-File Report 94-159, 60 p.
- Stanley, W.D., Johnson, S.Y., Qamar, A.I., Weaver, C.S., and Williams, J.M., 1996, Tectonics and seismicity of the southern Washington Cascade range: *Seismological Society of America Bulletin*, v. 86, no. 1A, p. 1–18.
- ten Brink, U.S., Molzer, P.C., Fisher, M.A., Blakely, R.J., Bucknam, R.C., Parsons, T., Crosson, R.S., and Creager, K.C., 2002, Subsurface geometry and evolution of the Seattle fault zone and Seattle basin, Washington: *Seismological Society of America Bulletin*, v. 92, p. 1737–1753, doi:10.1785/0120010229.
- Tréhu, A., Asudeh, I., Brocher, T.M., Luetgert, J.H., Mooney, W.D., Nabelek, J.L., and Nakamura, Y., 1994, Crustal architecture of the Cascadia forearc: *Science*, v. 266, p. 237–243, doi:10.1126/science.266.5183.237.
- Van Wagoner, T.M., Crosson, R.S., Medema, K.C., Preston, L., Symons, N.P., and Brocher, T.M., 2002, Crustal structure and relocated earthquakes in the Puget Lowland, Washington, from high-resolution tomography: *Journal of Geophysical Research*, v. 107, no. B12, p. 1–23, doi:10.1029/2001JB000710.
- Walsh, T.J., Korosec, M.A., Phillips, W.M., Logan, R.L., and Schasse, H.W., 1987, Geologic map of Washington—Southwest quadrant: Washington Division of Geology and Earth Resources Geologic Map GM-34, scale 1:250,000, 28 p.
- Walsh, T.J., Polenz, M., Logan, R.L., Lanphere, M.A., and Sisson, T.W., 2003, Pleistocene tephrostratigraphy and paleogeography of the southern Puget Sound near Olympia, Washington, in Swanson, T.W., ed., *Western Cordillera and Adjacent Areas*: Geological Society of America Field Guide 4, p. 225–236, doi:10.1130/0-8137-0004-3.225.
- Wells, R.E., and Coe, R.S., 1985, Paleomagnetism and geology of Eocene volcanic rocks of southwest Washington, implications for mechanisms of tectonic rotation: *Journal of Geophysical Research*, v. 90, p. 1925–1947, doi:10.1029/JB090iB02p01925.
- Wells, R.E., and Simpson, R.W., 2001, Northward migration of the Cascadia forearc in the northwestern U.S. and implications for subduction deformation: *Earth, Planets, and Space*, v. 53, p. 275–283, doi:10.1186/BF03352384.
- Wells, R.E., Weaver, C.S., and Blakely, R.J., 1998, Fore-arc migration in Cascadia and its neotectonic significance: *Geology*, v. 26, p. 759–762, doi:10.1130/0091-7613(1998)026<0759:FAMICA>2.3.CO;2.
- Wells, R.E., Bukry, D., Friedman, R., Pyle, R., Duncan, R., Haeussler, P., and Wooden, J., 2014, Geologic history of Siletzia, a large igneous province in the Oregon and Washington Coast Range: Correlation to the geomagnetic polarity time scale and implications for a long-lived Yellowstone hotspot: *Geosphere*, v. 10, p. 692–719, doi:10.1130/GES01018.1.